Romanian Reports in Physics **70**, 403 (2018)

INFLUENCE OF INITIAL SHAPE OF THREE-DIMENSIONAL FEW-CYCLE OPTICAL PULSE ON ITS PROPAGATION IN TOPOLOGICAL INSULATOR THIN FILMS

N.N. KONOBEEVA[1,a], M.B. BELONENKO[1,2,b]

[1] Volgograd State University, University Avenue 100, 400062, Volgograd, Russia
E-mail [a]: *yana_nn@volsu.ru*, E-mail [b]: *mbelonenko@yandex.ru*
[2] Volgograd Institute of Business, Uzhno-ukrainskaya str. 2, 400002, Volgograd, Russia

Received September 29, 2017

Abstract. We consider the propagation of three-dimensional few-cycle optical pulses in topological insulator thin films within the framework of an effective long-wave Hamiltonian in the case of low temperature. The key features of the propagation dynamics of input Gaussian, Bessel, and Airy pulse shapes are revealed.

Key words: few-cycle pulses, topological insulator, input pulse shape.

1. INTRODUCTION

A topological insulator means any system with an energy gap in the spectrum (in the case of an electron in the bulk of the sample), but with gapless states on the surface. A necessary condition for the existence of a phase of a topological insulator is, on the one hand, the presence of a strong spin-orbit interaction [1, 2], and on the other hand, the presence of symmetry with respect to inversion of time. Despite the increase in the number of publications in this area, the question of the interaction of this system with the field of a few-cycle optical pulse, which has broad and promising areas of applications, remains open.

Among nonlinear optical phenomena, few-cycle optical pulses [3], representing pulses from several oscillations of the electric field, are of great interest to researchers [4–24]. In this paper, along with the typical Gaussian pulse, the Bessel pulse is investigated, as well as a new type of optical pulse, which has become popular among light beams – the Airy pulse. These space-time waves have a unique property of non-diffraction, *i.e.* propagate (in the absence of non-linearity), without diffraction or dispersion. This class of universal waves can be used in ultra-fast sounding or for visualization in environments with poorly studied or dynamically changing properties.

2. BASIC EQUATIONS

The energy spectrum for thin film topological insulators can be written in the following form [25]:

$$\varepsilon(p_x, p_y) = (p_x^2 + p_y^2)/2m + v_f\sqrt{p_x^2 + p_y^2}, \tag{1}$$

where p_x, p_y are the components of the electron momentum, m is the effective electron mass, σ_x, σ_y are the spin matrices, and v_f is the Fermi velocity.

Following the general concepts of quantum mechanics, in the presence of an external electrical field E directed along the x axis, without loss of generality, choosing the gauge field: $E = -\partial A / c\partial t$ (c is the light velocity), we need to change the momentum to a generalized momentum: $p \to p - eA/c$ (e is the electron charge). In this case, the Hamiltonian for the topological insulator can be written as follows:

$$H = \sum_{p\sigma} \varepsilon(p - \frac{e}{c}A(t)) a_{p\sigma}^{+} a_{p\sigma}, \tag{2}$$

where $a_{p\sigma}^{+}, a_{p\sigma}$ are the creation and annihilation operators of the electron with the quasimomentum p and spin σ.

In the three-dimensional case, the Maxwell's equations have the form:

$$\frac{\partial^2 \mathrm{A}}{\partial x^2} + \frac{\partial^2 \mathrm{A}}{\partial y^2} + \frac{\partial^2 \mathrm{A}}{\partial z^2} - \frac{1}{c^2}\frac{\partial^2 \mathrm{A}}{\partial t^2} + \frac{4\pi}{c}\Phi(\mathrm{A}) = 0, \tag{3}$$

where A is the vector potential, $\boldsymbol{A} = (0, A(x, y, z, t), 0)$.

Let us write the standard expression for the current density:

$$j = e\sum_{p} v_y(p - \frac{e}{c}A(x, y, z, t))\langle a_p^{+} a_p \rangle, \tag{4}$$

where $v_y(p) = \dfrac{\partial\varepsilon(p_x, p_y)}{\partial p_y}$, and the brackets show averaging with a nonequilibrium density matrix $\rho(t)$: $\langle B \rangle = Sp(B(0)\rho(t))$. Taking into account that $[a_p^{+} a_p, H] = 0$, the equation of motion for the density matrix easily provides:

$\left\langle a_p^+ a_p \right\rangle = \left\langle a_p^+ a_p \right\rangle_0$, where $\left\langle B \right\rangle_0 = Sp(B(0)\rho(0))$. So, in the expression for the electric current, we can use the particle number calculated from the Fermi-Dirac distribution. Further, we will consider the case of low temperature where only a small area of the momentum space near the Fermi level gives nonzero contribution into the sum (or integral) of (4):

$$j = e\int_{-\Delta}^{\Delta}\int_{-\Delta}^{\Delta} \mathrm{d}p_x \mathrm{d}p_y v_y (p - \frac{e}{c} A(x,t)). \tag{5}$$

The integration limits are determined from the condition that the number of particles be equal:

$$\int_{-\Delta}^{\Delta}\int_{-\Delta}^{\Delta} \mathrm{d}p_x \mathrm{d}p_y = \int_{ZB} \mathrm{d}p_x \mathrm{d}p_y \left\langle a_{px,py}^+ a_{px,py} \right\rangle.$$

The integration on the right hand side is over the Brillouin zone.

Then we can write the equation for the three-dimensional (3D) few-cycle optical pulse propagation as follows:

$$\begin{aligned}
&\frac{\partial^2 \mathrm{A}}{\partial x^2} + \frac{\partial^2 \mathrm{A}}{\partial y^2} + \frac{\partial^2 \mathrm{A}}{\partial z^2} - \frac{1}{c^2}\frac{\partial^2 \mathrm{A}}{\partial t^2} + \frac{4\pi}{c}\Phi(\mathrm{A}) = 0 \\
&\Phi(A) = e[\phi(\Delta - e/cA, \Delta) - \phi(\Delta - e/cA, -\Delta) \\
&\qquad - \phi(-\Delta - e/cA, \Delta) + \phi(-\Delta - e/cA, -\Delta)] \\
&\phi(x,y) = y^2 x/2m + x^3/6m + v_F x(x^2 + y^2)^{1/2}/2 + v_F y^2 \ln(x + (x^2 + y^2)^{1/2})/2.
\end{aligned} \tag{6}$$

In the cylindrical coordinate system, the equation (6) has the form:

$$\mathrm{A}_{tt} = \frac{1}{r}\frac{\partial}{\partial r}\left(r\frac{\partial \mathrm{A}}{\partial r}\right) + \frac{\partial^2 \mathrm{A}}{\partial z^2} + \frac{1}{r^2}\frac{\partial^2 \mathrm{A}}{\partial \varphi^2} + 4\pi\Phi(\mathrm{A}). \tag{7}$$

Assuming that the system is axisymmetric, we have $\partial/\partial\varphi \to 0$. Due to the field inhomogeneity along a certain axis, the resulting current is inhomogeneous, thereby leading to a charge accumulation in some areas. From the charge conservation law, one can conclude that the duration of the ultra-short pulse will have a significant impact on the accumulated charge:

$$\partial\rho/\partial t + \partial j/\partial x = 0, \quad \rho \propto \tau\frac{j}{l_x}. \tag{8}$$

Here ρ is the charge density, j is the current density along the x axis, τ is the pulse duration, l_x is the characteristic length at which the electric field of the pulse changes along the x axis.

The equation (8) allows us to conclude that the pulse duration has a significant effect on the accumulated charge. Our estimations – the stored charge being about 1–2% of the charge contributing to the current – suggest that the charge accumulation effect for femtosecond pulses can be ignored. This is confirmed by the numerical experiments for the case of carbon nanotubes and pulses with a duration of tens of femtoseconds [26].

3. MAIN RESULTS

The equation (7) is solved numerically [27]. The initial conditions are chosen in three forms: Gaussian beam (9a), Bessel pulse (9b), and Airy pulse (9c):

$$\begin{aligned} A(z,r,0) &= Q\cdot\exp\left(-\left(\frac{z-z_0}{\gamma_z}\right)^2\right)\exp\left(-\frac{r^2}{\gamma_r}\right) \\ \frac{\mathrm{d}A(z,r,0)}{\mathrm{d}t} &= 2Q\nu_z\frac{(z-z_0)}{\gamma_z^2}\exp\left(-\left(\frac{z-z_0}{\gamma_z}\right)^2\right)\exp\left(-\frac{r^2}{\gamma_r}\right) \end{aligned} \tag{9a}$$

$$\begin{aligned} A(z,r,0) &= Q\exp\left(-\left(\frac{z-z_0}{\gamma_z}\right)^2\right)J_0\left(\frac{r}{\gamma_r}\right)\exp\left(-\frac{r}{\gamma_r}\right) \\ \frac{\mathrm{d}A(z,r,0)}{\mathrm{d}t} &= 2Q\nu_z\frac{(z-z_0)}{\gamma_z^2}\exp\left(-\left(\frac{z-z_0}{\gamma_z}\right)^2\right)J_0\left(\frac{r}{\gamma_r}\right)\exp\left(-\frac{r}{\gamma_r}\right) \end{aligned} \tag{9b}$$

$$\begin{aligned} F(x) &= \int_x^\infty Ai(y)\mathrm{d}y \\ A(z,r,0) &= QF\left(\frac{z-z_0}{\gamma_z}+\kappa\left(\frac{z-z_0}{\gamma_z}\right)^2\right)J_0\left(\frac{r}{\gamma_r}\right)\exp\left(-\frac{r}{\gamma_r}\right) \\ \frac{\mathrm{d}A(z,r,0)}{\mathrm{d}t} &= Q\left.\frac{\mathrm{d}F\left(\frac{z-z_0-\nu_z\cdot t}{\gamma_z}+\kappa\left(\frac{z-z_0-\nu_z\cdot t}{\gamma_z}\right)^2\right)}{\mathrm{d}t}\right|_{t=0} J_0\left(\frac{r}{\gamma_r}\right)\exp\left(-\frac{r}{\gamma_r}\right) \end{aligned} \tag{9c}$$

where r is the radius, Q is the amplitude, γ_z, γ_r determine the width of the pulse in the z- and r-directions, respectively, z_0 is the initial coordinate of the pulse center; v_z is the initial pulse velocity along the z axis; κ is the parameter that determines the type of the Airy beam and is related by the dispersion coefficient in a linear medium [28]; $Ai(y)$ is the Airy function.

Note that the pulse with initial conditions (9b) (*i.e.* the Bessel beam) was cut off, with the characteristic cutoff parameter γ_r. This is due to the physically unrealizable pulse because of the infinity of its energy. The values of energy parameters are expressed in units of Δ. Note that the time is chosen as the evolution variable.

The evolution of a 3D electromagnetic field with the initial conditions (9a) as it propagates along the sample is shown in Fig. 1.

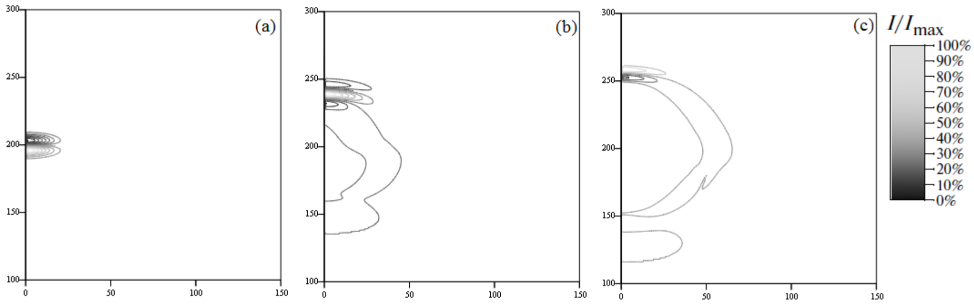

Fig. 1 – The intensity of 3D electromagnetic pulse $I(r, z, t) = E^2(r, z, t)$ at different values of time: a) the initial pulse shape; b) $t = 5\cdot10^{-13}$ s; c) $t = 7\cdot10^{-13}$ s.

It can be seen that the pulse propagates steadily, with a slight spreading and a loss in amplitude. This behavior on the one hand is due to dispersion, which leads to broadening of the optical pulse, and on the other hand, is due to the nonlinearity of equation (7), which determines its "narrowing". Thus, the stable propagation of the pulse is possible due to the balance between these two processes in the topological insulator.

The dynamics of propagation of a pulse along a sample as a function of the initial conditions (9b, 9c) is illustrated in Fig. 2.

As can be seen from Fig. 2, the Gaussian pulse and the Bessel pulse propagate most stably with the amplitude of the main peak retained. The Airy pulse spreads under the same conditions, essentially losing amplitude. This is due precisely to the presence of nonlinearity in the system under consideration.

For a more detailed study of the evolution of the pulse shape, we construct the dependence of the electric field of the pulse on the radius for different instants of time in the direction of propagation of the Bessel beam and along the radius for the Airy pulse; see Fig. 3 and Fig. 4.

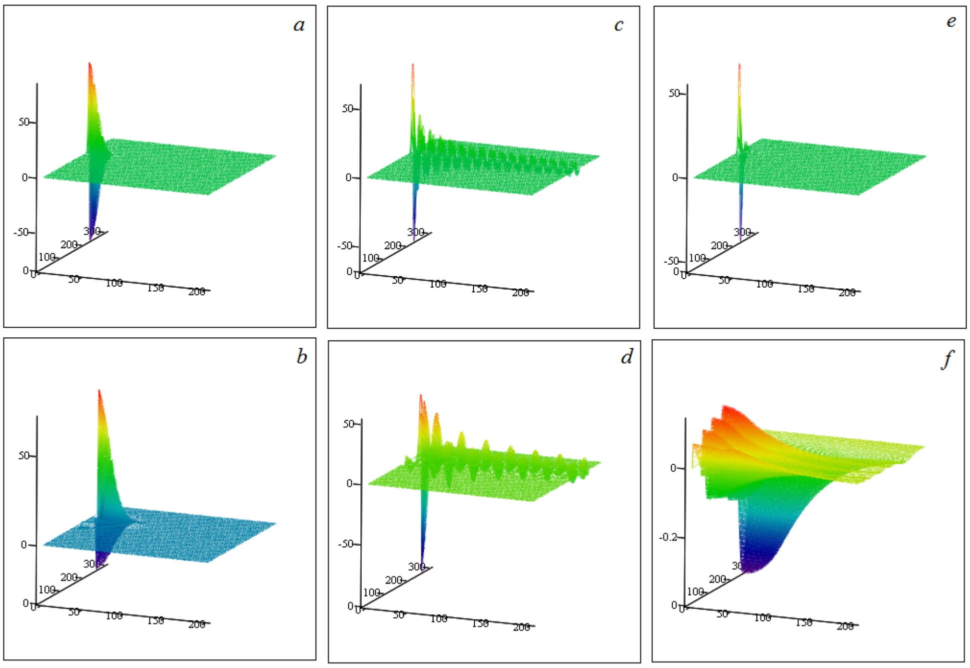

Fig. 2 – The amplitude of the 3D electromagnetic pulse at different values of the time: a), c), e) the initial shape; b), d), f) $t = 5 \cdot 10^{-13}$ s. Figs. a,b correspond to the initial conditions (9a), Figs. c,d – (9b), Figs. e,f – (9c).

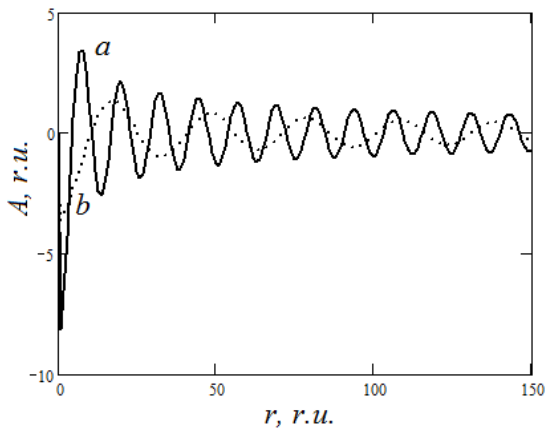

Fig. 3 – The dependence of the electric field for the Bessel pulse on the radius in the direction of the pulse propagation: a) $t = 0$; b) $t = 5 \cdot 10^{-13}$ s.

As follows from the dependence shown in Fig. 3, the Bessel pulse propagates through a thin film of a topological insulator rather stably, experiencing only a loss in the amplitude of about 2 times, but retaining its shape.

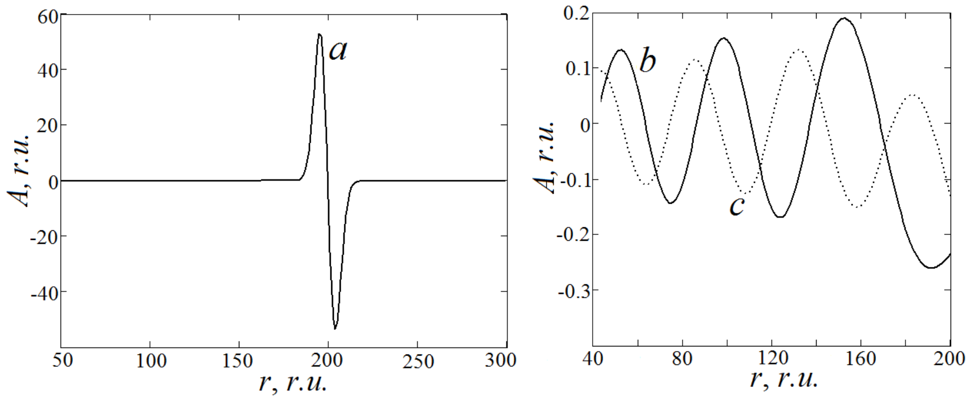

Fig. 4 – A portion of the dependence of the electric field for the Airy pulse on the radius in the direction along the radius: a) $t = 0$; b) $t = 1\cdot10^{-13}$ s; c) $t = 5\cdot10^{-13}$ s.

In Fig. 4, the graph (a) is taken apart, since the pulse exceeds 10 times the amplitude in (b, c). It is obvious that the pulse significantly changes its shape when propagating over the sample in comparison with the initial instant of time. It can be concluded that, in contrast to linear media, it is necessary to determine completely different pulse shapes in nonlinear media for stable propagation.

An important question is also the stability of the obtained solutions with respect to perturbations that depend on the angle ϕ. The stability analysis can be carried out on the basis of the linearized equation (7), which for small perturbations δA will have the form:

$$\delta A_{tt} = \frac{1}{r}\left(r\frac{\partial \delta A}{\partial r}\right) + \frac{\partial^2 \delta A}{\partial z^2} + \frac{1}{r^2}\frac{\partial^2 \delta A}{\partial \phi^2} + 4\pi\frac{\partial j(A)}{\partial A}\delta A. \qquad (10)$$

We note that the last term in (10) is calculated on the solutions $A(z, r, t)$ of equation (7). Because of the linearity of (10), one can search for δA as:

$$\delta A \propto \delta A(z,r,t)\exp(\mathrm{i}m\phi). \qquad (11)$$

Next, we can calculate the corresponding corrections to the electric field:

$$\delta E = -c^{-1}\partial \delta A / \partial t.$$

The corresponding results for the electric field are presented in Fig. 5 and Fig. 6. These figures show the maximum magnitude modulus δE (throughout the calculation area) as a function of time (Fig. 5) and number *m* (Fig. 6).

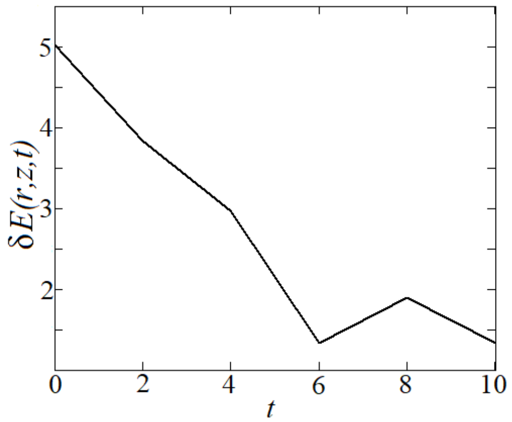

Fig. 5 – Dependence of maximum modulus $E(r, z, t)$ on time t (1 r.u. = 10^{-12} s).

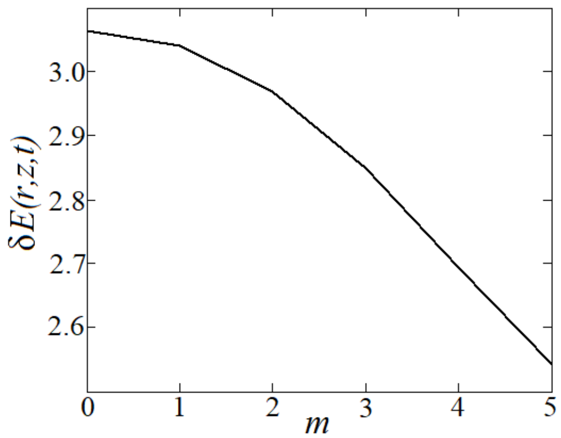

Fig. 6 – Dependence of maximum $\delta E(r, z, t)$ on m.

Figure 5 shows that the perturbations decrease with time. The dip in the graph in the region $6 \cdot 10^{-12}$ s is associated with the formation of a nonlinear focus and a change in the shape of the pulse. According to Fig. 6 (calculations are made for one instant of time), the faster the perturbation decreases, the larger the number *m* is. These results allow us to conclude that the obtained solutions are stable to the angular perturbations.

4. CONCLUSIONS

The results reported in this paper show that a stable propagation of three-dimensional few-cycle optical pulses in thin film topological insulators in the case of initial pulse profiles in the form of Gauss or Bessel profiles is possible. In the case of Airy pulse profiles, stable propagation is not observed. This effect can be useful in the development of hybrid devices based on the effect of light interaction with the electrons of a topological insulator.

Acknowledgments. This work was supported by the Ministry for Education and Science of the Russian Federation under the project No. MK-4562.2016.2, government task No. 2.852.2017/4.6.

REFERENCES

1. S. Murakami, N, Nagaosa, and S.-C. Zhang, Phys. Rev. Lett. **93**, 156804 (2004).
2. B.A. Bernevig, T.L. Huges, and S.-C. Zhang, Science **314**, 1757–1761 (2006).
3. V.N. Vlasov, I.A. Petrischev, and V.I. Talanov, Radiophys. Quantum Electron. **14**, 1062–1070 (1971).
4. Y. Silberberg, Opt. Lett. **15**, 1282–1284 (1990).
5. I.V. Mel'nikov, H. Leblond, F. Sanchez, and D. Mihalache, IEEE J. Select. Top. Quantum Electron. **10** (5), 870–875 (2004).
6. H. Leblond, I.V. Mel'nikov, and D. Mihalache, Phys. Rev. A **78** (4), 043802 (2008).
7. H. Leblond and D. Mihalache, Phys. Rev. A **79** (6), 063835 (2009).
8. Y.S. Kivshar and B.A. Malomed, Rev. Mod. Phys. **61** (4), 763–915 (1989).
9. D.N. Neshev, T.J. Alexander, E.A. Ostrovskaya, Y.S. Kivshar, H. Martin, I. Makasyuk, Z. Chen, Phys. Rev. Lett. **92** (12), 123903 (2004).
10. D. Neshev, E. Ostrovskaya, Y. Kivshar, and W. Krolikowski, Opt. Lett. **28** (9), 710–712 (2003).
11. J.S.T. Gongora, A.E. Miroshnichenko, Y.S. Kivshar, and A. Fratalocchi, Nature Commun. **8**, 15535 (2017).
12. J.S. Huang and Y. Kivshar, ACS Photonics **3** (8), 1333–1335 (2016).
13. R.S. Savelev, A.V. Yulin, A.E. Krasnok, and Y.S. Kivshar, Days on Diffraction (DD) **2016**, 367–372 (2016).
14. M.A. Karpierz, M. Sierakowski, M. Swillo, and T. Wolinski, Mol. Cryst. Liq. Cryst. **320**, 157–163 (1998).
15. M. Warenghem, J.F. Henninot, and G. Abbate, Mol. Cryst. Liq. Cryst. **320**, 207–230 (1998).
16. M. Warenghem, J.F. Henninot, and G. Abbate, Opt. Exp. **2**, 483–490 (1998).
17. M. Pecciani, A. De Rossi, G. Assanto, A. De Luca, C. Umeton, and I.C. Khoo, Appl. Phys. Lett. **77** (1), 7–9 (2000).
18. T. Brabec and F. Krausz, Rev. Mod. Phys. **72**, 545–591 (2000).
19. A.I. Maimistov, Quantum Electronics **30**, 287–304 (2000).
20. H. Leblond and D. Mihalache, Phys. Rep. **523**, 61–126 (2013).
21. D.J. Frantzeskakis, H. Leblond, and D. Mihalache, Rom. J. Phys. **59**, 767–784 (2014).
22. S.V. Sazonov, Opt. Commun. **380**, 480–491 (2016).
23. D. Mihalache, Rom. Rep. Phys. **69**, 403 (2017).
24. S.V. Sazonov and N.V. Ustinov, JETP **124**, 213–230 (2017).

25. S. Basak, H. Lin, L.A. Wray, S.-Y. Xu, L. Fu, M.Z. Hasan, and A. Banzil, Phys. Rev. B **84**, 121401 (2011).
26. A.V. Zhukov, R. Bouffanais, E.G. Fedorov, and M.B. Belonenko, J. Appl. Phys. **114**, 143106 (2013).
27. J.W. Thomas, *Numerical partial differential equations-finite difference methods*, Springer-Verlag, New York, 1995.
28. V.H. Chong, D.N. Christodoulides, and F.W. Wise, Nature Photon. **4**, 103–106 (2010).